JOURNAL OF GEOPHYSICAL RESEARCH, VOL. 101, NO. D3, PAGES 7209–7225, MARCH 20, 1996

The land surface-atmosphere interaction: A review based on observational and global modeling perspectives

Alan K. Betts and John H. Ball
Atmospheric Research, Pittsford, Vermont

Anton C. M. Beljaars, Martin J. Miller and Pedro A. Viterbo
European Centre for Medium-Range Weather Forecasts, Reading, England

Abstract. This review discusses the land-surface-atmosphere interaction using observations from two North American field experiments (First International Satellite Land Surface Climatology Project Field Experiment (FIFE) and Boreal Ecosystem Atmosphere Study (BOREAS)) and the application of research data to the improvement of land surface and boundary layer parameterizations in the European Centre for Medium-Range Weather Forecast (ECMWF) global forecast model. Using field data, we discuss some of the diurnal and seasonal feedback loops controlling the net surface radiation and its partition into the surface sensible and latent heat fluxes and the ground heat flux. We consider the impact on the boundary layer evolution and show the changes in the diurnal cycle with soil moisture in midsummer. We contrast the surface energy budget over the tropical oceans with that over both dry and wet land surfaces in summer. Results from a new ECMWF model with four predicted soil layers illustrate the interaction between the soil moisture reservoir, evaporation and precipitation on different timescales and space scales. An analysis of an ensemble of 30-day integrations for July 1993 (the month of the Mississippi flood) showed a large sensitivity of the monthly precipitation pattern (and amount) to different initial soil moisture conditions. Short-range forecasts with old and new land surface and boundary layer schemes showed that the new scheme produced much better precipitation forecasts for the central United States because of a more realistic thermodynamic structure, which in turn resulted from improved evaporation in an area that is about 1-day upstream. The results suggest that some predictability exists in the extended range as a result of the memory of the soil moisture reservoir. We also discuss briefly the problem of soil moisture initialization in a global forecast model and summarize recent experience with nudging of soil moisture at ECMWF and improvements in the surface energy budget coming from the better prediction of clouds.

1. Introduction

This review discusses, in the context of the Global Energy and Water Experiment (GEWEX) Continental Scale International Project (GCIP), some recent research on the land surface-atmosphere interaction over the North American continent based on observational and model studies. We shall first review some of the physics of the land surface-atmosphere interaction using data from the First ISLSCP (International Satellite Land Surface Climatology Project) Field Experiment (FIFE) [*Sellers et al.*, 1992], and the Boreal Ecosystem Atmosphere Study (BOREAS) [*Sellers et al.*, 1995]. We then discuss the application of research data to the validation and improvement of near-surface parameterizations in global forecast models. These forecast model studies have further deepened our appreciation of the importance of the surface boundary condition over land in controlling weather and climate on different timescales. Over the oceans, the surface boundary condition represented by the sea surface temperature (SST) is well known to play a major role in forcing the atmosphere, but understanding its role has been a simpler task, both because SST is observed daily and because the surface is saturated at this temperature. In contrast, over land the temperature and moisture of the soil are not routinely observed or input daily as a boundary condition into global forecast models. Instead, they must be calculated from solving a full system of parameterized equations at the surface involving the surface radiation budget (strongly influenced by the solar diurnal cycle, and the model representation of the cloud field), the conduction of heat into the ground (an issue avoided over the oceans in models where SST is not calculated), the partition of the surface available energy into latent heat (evaporation) and sensible heat transfers to atmosphere, as well as the surface layer and boundary layer parameterizations (a common issue with the ocean surface). In turn this partition, which controls the surface Bowen ratio (BR), depends on evaporation from bare ground, from wet vegetation (after recent precipitation), and evapotranspiration by the ecosystem of crops, grassland, or forests. Evapotranspiration draws water from deeper root zones in the soil (and different plant species have different rooting depths), so that the surface evaporation, which ultimately controls the surface energy partition, and the evolution of the atmospheric boundary layer (BL) depend on the subsurface hydrology (the infiltration of precipitation and its redistribution within the soil, the subsurface drainage, the drainage associated

Paper number 95JD02135.
0148-0227/96/95JD-02135$05.00

with the topography, and the runoff into streams and rivers). All these near-surface processes are parameterized in global models, and the surface fluxes of heat and water to the atmosphere are at the end of this chain of parameterizations, which include the hydrology, precipitation, cloud field, vegetation, radiation field, surface layer, and boundary layer.

The impact of land surface processes in general circulation models has been reviewed recently by *Garratt* [1993]. Included in the studies he cites are papers by *Rowntree and Bolton* [1983], *Dickinson and Henderson-Sellers* [1988], *Nobre et al.* [1991], *Lean and Rowntree* [1993], *Atlas et al.* [1993] and *Milly and Dunne* [1994]. Of particular importance is the review by *Mintz* [1984], who concluded that a coupling exists between evaporation and precipitation, in the sense that precipitation increases over land when evaporation increases. This implies a positive feedback from the recirculation of precipitation through the soil moisture reservoir, which may lead to prolonged persistence of anomalous wet or dry spells. Such a persistence was indeed found by *Oglesby* [1991] from model simulations and suggested earlier in a data study by *Namias* [1958], in which significant lagged correlations were found in the 700-hPa field over the Midwestern United States between spring and summer, and from a correlation of spring precipitation anomalies and summer temperature anomalies.

Although the precipitation response to evaporation is marked, it is not very clear how this response works in detail. *Rowntree and Bolton* [1983] present the general notion that evaporation increases the moisture content of the troposphere and brings the air closer to saturation and therefore closer to precipitation. However, soil moisture only affects the partitioning of sensible and latent heat flux at the surface. Consequently, the surface flux of equivalent potential temperature (θ_e , which determines the moist adiabat for convective precipitation) into the boundary layer is not directly affected by the surface Bowen ratio. *Betts et al* [1994] and *Betts and Ball* [1995] demonstrate with the help of FIFE data and a simple boundary layer model that the reduced evaporation, and therefore increased heating at the surface, increases the entrainment at the top of the boundary layer, and therefore increases the entrainment of low-θ_e air from above the boundary layer. This leads to a lower afternoon θ_e in the boundary layer, a more stable troposphere, and might therefore lead to less convective precipitation. In particular, a lower θ_e over a continent might lead to reduced precipitation over that continent in relation to the surrounding ocean. However, studies of the summer precipitation over the Mississippi basin have shown that in this region two boundary layers are involved. The summer precipitation is closely linked to a persistent flow pattern, sometimes referred to as the U.S. summer monsoon. The moisture comes from the Gulf of Mexico in a northward boundary layer flow over Mexico, Texas, and Oklahoma, curving gradually eastward over the plains [*Rasmusson*, 1968, 1971]. Precipitation is often the result of severe storms, which are triggered by upper air disturbances coming from the west. *Benjamin and Carlson* [1986] and *Lanicci et al.* [1987] propose another mechanism for the control of precipitation by upstream surface evaporation. They demonstrate that the warm air coming from the plateau of Mexico with a southwesterly wind puts a lid on the moist air coming from the south from the Gulf of Mexico. The differential advection plays a crucial role in this mechanism. When the soil is more moist over the Mexican plateau the heating is smaller, the capping inversion is weaker, and convective precipitation is not inhibited.

The second topic of this paper is the development of improved forecast models, and in particular the European Centre for Medium-Range Forecasting (ECMWF) model. Over land, only air temperature and humidity, wind and precipitation are measured synoptically, and these have long been used as measures of the accuracy of forecast products. Recently, data from the FIFE experiment were used to directly identify systematic errors in the model parameterizations over land [*Betts et al.*, 1993]. Data from this and other field programs were then used to develop improved land surface and boundary layer parameterizations for the ECMWF model [*Viterbo and Beljaars*, 1995]. Results from the new model illustrate the interactions discussed above between the soil moisture reservoir, evaporation, and precipitation on different timescales and space scales. An analysis of an ensemble of 30-day integrations for July 1993 (the month of the Mississippi flood) showed a large sensitivity of the monthly precipitation amount and pattern to different initial soil moisture conditions [*Beljaars et al.*, 1995]. Short-range forecasts with old and new land surface and boundary layer schemes showed that the new scheme produced much better precipitation forecasts for the central United States due to a more realistic thermodynamic structure, which in turn resulted from improved evaporation in an area that is about one day upstream, in agreement with the observational studies cited above.

Finally, this review briefly discusses the problem of soil moisture initialization in a global forecast model, and summarizes recent experience with nudging of soil moisture in the ECMWF model. In general, the results suggest that improved predictability exists in both short and extended range forecasting, due to the memory of the soil moisture reservoir.

2. Physical Processes

Figure 1 summarizes some of the important feedback loops for the land surface-atmosphere interaction; those we shall refer to in this review. We distinguish a diurnal loop (heavy solid lines) and a longer timescale "seasonal" loop (heavy dashed lines) associated with the longer timescale memory of soil temperature and moisture. A "century" timescale loop between

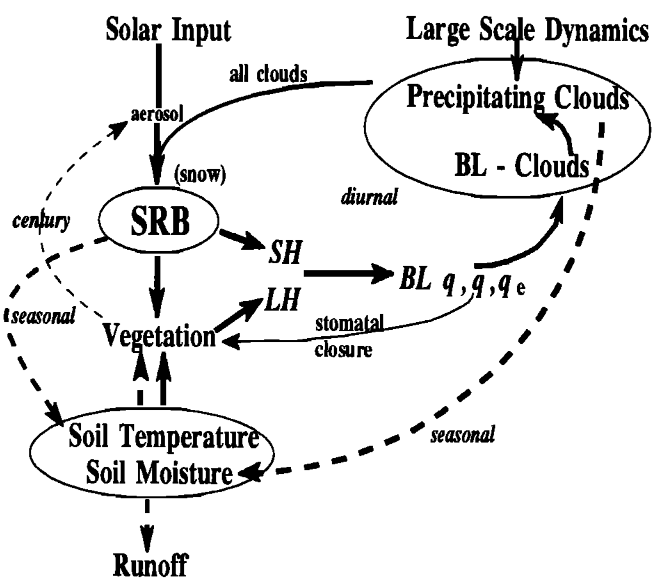

Figure 1. Schematic showing some important land surface-atmosphere interactions on different timescales.

vegetation and aerosol has been indicated as a light dashed line as a reminder of the periodic burning of forests, which add aerosol to the atmosphere and reduce the incoming net radiation. The light line marked stomatal closure is the vegetative control on evaporation in warm dry atmospheric conditions. We will discuss the components of Figure 1 in sequence, starting with the surface radiation budget (SRB) which drives the strong diurnal surface cycle over land. Then we discuss the partition of the SRB into the sensible (SH) and latent heat (LH) fluxes, which drive the diurnal cycle of the boundary layer (BL), often producing clouds and sometimes precipitation.

2.1. Surface Radiation Budget

The solar terms are the dominant terms in this budget, at least during the daytime and in summer. Reflection and absorption by clouds and aerosol reduce the incoming solar radiation at the surface; while the surface albedo varies from as little as 8% for northern conifer forests to 80% for fresh snow over grassland. Figure 2 shows the seasonal variation of albedo using data from the BOREAS experiment in Canada for 2 grassland sites (solid lines), a deciduous aspen site (light dashes) and 2 conifer sites (one of jack pine (heavy dashed) and one mostly spruce (dotted)). The data are 15-day averages plotted against Julian day for 1994. The five sites are at Saskatoon (SK), Meadow Lake (MD), Prince Albert Park (PA), Thompson (TH), and a stand of old jack pine (OJP) west of Thompson. In winter, the albedo is as high as 80% over snow on grassland (generally less over the forests, where snow does not stay long on the canopy). One consequence is that the incoming net radiation is near zero even in the daytime over snow covered grassland in midwinter. The higher summer albedo of grassland (20%) means that the energy available for transfer to the atmosphere as sensible heat and latent heat is reduced. The albedo of the deciduous aspen increase with leafup from a minimum of 11% in the spring to about 16% in midsummer. In summer, the conifers have the lowest albedo. The curve near 10% is for a stand of jack pine, while the lower curve near 8% is a more dense canopy of mostly spruce. The

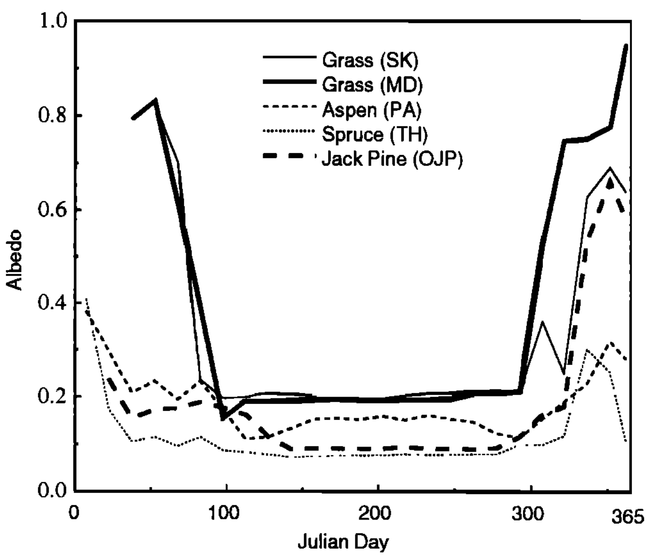

Figure 2. Seasonal variation of albedo for forest and grassland sites in Boreal Ecosystem Atmosphere Study (BOREAS) in 1994.

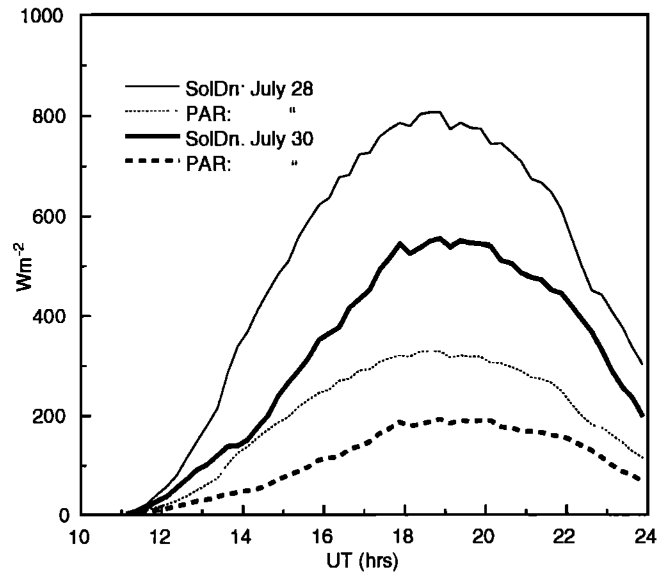

Figure 3. Reduction of incoming Solar radiation and Photosynthetically Active radiation by smoke aerosol from forest fires near Thompson, Manitoba, between a clear day (July 28) and a smoky day (July 30, 1994).

difference in albedo between forest and grassland has been shown to have an important impact on precipitation in models because of the greater absorption of energy at the surface (e.g. *Mylne and Rowntree*, [1991] and for the grassland to desert transition, see *Charney et al.*, [1977].

There is a long timescale feedback loop between vegetation, fires, aerosol and surface radiation budget (SRB), which is indicated schematically by the light dashed line in Figure 1 linking vegetation and aerosol. The northern Boreal forests burn every century or so, and the fires occur preferentially in dry summers These fires reverse the uptake of carbon from the atmosphere, which occurs over long time periods during photosynthesis driven by the incoming photosynthetically active radiation (PAR). The smoke aerosol reduces PAR at the surface. Figure 3 illustrates the impact of smoke aerosol from burning forest fires over northern Manitoba on the incoming solar radiation (SolDn) and PAR at Thompson, Manitoba. The data is again from BOREAS in 1994. The fires were about 100 km from the measurement site: July 28 (light curves) was cloud free and relatively smoke free, while on July 30 (heavy curves) the northwest prevailing wind, carrying smoke from the forest fires, reduced the total incoming solar radiation by about 32% and the incoming PAR by 42%. The percent reduction in PAR is greater because the smoke aerosol is a stronger absorber in the visible PAR spectral band. Over the northern forests smoke aerosol may exert a significant climatic impact on the SRB, although this will need careful quantitative assessment. It is likely that even forecast models will have to include a prognostic equation for aerosol, because of its importance in the SRB. In this admittedly extreme example, of July 30 1994 in Thompson, the global model forecast temperature was high by several degrees at local noon.

Indeed, it is difficult to calculate the SRB to sufficient accuracy in global forecast and climate models. Many models underestimate the absorption or reflection of solar energy in the atmosphere, either by clouds or aerosol or other absorption processes that are poorly modeled, with the result that they overestimate the incoming short wave radiation at the surface [e.g., *Garratt et al.*, 1993; *Betts et al.*, 1993; *Cess et al.*, 1995]. *Ramanathan et al.* [1995] have discussed the impact of higher absorption by clouds on the tropical ocean budget, but overestimation of the incoming solar radiation over land also has major impact on the climate over land [*Garratt et al.*, 1993]. *Viterbo and Courtier* [1995] found that excessive net radiation at the surface (due primarily to model underestimates of cloud) forced excessive surface evaporation, and dried out the soil moisture during data assimilation in the ECMWF global model (see section 4.1).

2.2. Surface Energy Budget

Typically net radiation (Rnet) during the daytime heats the land surface. Some energy (G) is absorbed in the biomass and the soil (≤15%), while the majority is transferred back to the atmosphere as sensible and latent heat. The key issue over land is the partition of this available surface energy (Rnet-G) into sensible (SH) and latent heat (LH) fluxes. The surface Bowen ratio (BR=SH/LH)) varies widely over land: it depends on temperature, the availability of water for evaporation, the entrainment of dry air into the boundary layer (BL) from above and vegetative controls at the surface (see section 2.3). Climatologies exist [e.g., *Henning*, 1989], but the surface BR is poorly known because routine measurements of this flux partition are sparse. At the extreme of the desert, where water for evaporation is very limited, most of the transfer to the atmosphere occurs as SH, which warms a deep but dry boundary layer. (Over deserts, Rnet itself may be reduced significantly by the large net outgoing longwave radiation [*Pielke*, 1984]) If water is readily available for evaporation (either on the surface or if the roots of vegetation have access to water in the soil), as much as 75-80% of the total daytime transport of energy to the atmosphere occurs as latent heat. This evaporation keeps a moist land surface relatively cool. Thus in the daytime over the grassland FIFE sites with moist soils, the BR≈0.3 [*Kanemasu et al.*, 1992; *Smith et al.*, 1992], while at night the fluxes are smaller with SH flux downward and LH upward and a BR≈-1. The extreme case is deep open water. Over the ocean where SST changes little in response to the solar forcing (except with light winds), the mean surface BR is typically of order 0.07 at tropical temperatures. The equilibrium SH transfer to the atmosphere is then largely controlled by the radiative cooling of the shallow subcloud layer [*Betts and Ridgway*, 1989], which destabilizes the ocean-atmosphere interface.

The partition between SH and LH depends directly on temperature through the dependence of saturation vapor pressure on temperature but a realistic formulation of this effect on the BR over land has been elusive. *Priestley and Taylor* [1972], *McNaughton* [1976], and *Monteith* [1981] discussed how the assumption of a constant specific humidity deficit at the surface led to the definition of an "equilibrium" evaporation. These analyses have been extended by many others to include the effect of the mixing down of dry air into the boundary layer by entrainment [*Brutsaert*, 1976; *De Bruin*, 1983; *Jarvis and McNaughton*, 1986; *McNaughton and Spriggs*, 1986; *Culf*, 1994]. This increases surface evaporation (in the absence of a negative vegetative response). Betts (1994) showed that this mixed layer equilibrium evaporation problem could be formulated differently in terms of the balance between the tendencies produced by the surface fluxes and the entrainment fluxes at mixed-layer top (or cloud base) on the mixed layer saturation pressure (or lifting condensation level

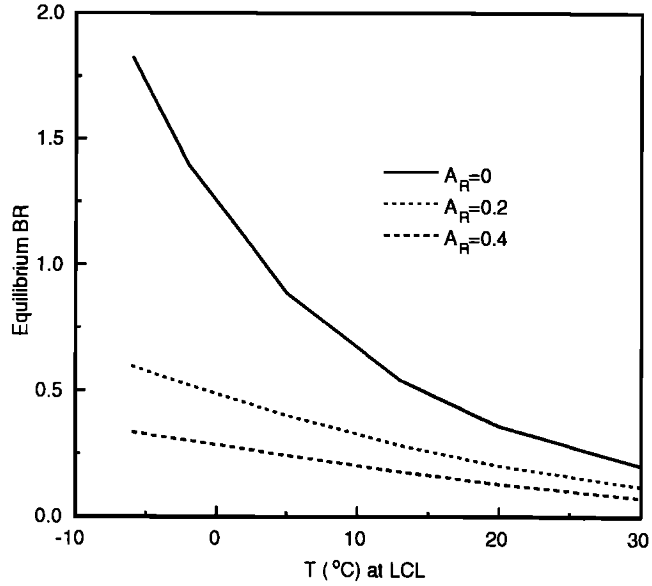

Figure 4. Equilibrium Bowen ratio as a function of temperature at the lifting condensation level (LCL) without entrainment (A_R=0) and for two entrainment rates.

(LCL)). Figure 4 summarizes this definition of an "equilibrium" surface BR as a function of temperature at the LCL for different entrainment rates at mixed-layer top. Entrainment is represented by a closure parameter A_R on the buoyancy flux [*Stull*, 1988]. A value of A_R=0 represents no entrainment; A_R=0.2 has been widely used in mixed layer models and A_R=0 4 is the higher value estimated from FIFE data (see section 2.6 later). The curves are drawn for one LCL at 850 mbar, since the dependance on saturation pressure is weak in comparison with the temperature dependence. The upper solid curve shows the strong dependence of equilibrium surface BR on temperature alone. The lower curves show the effect of increasing entrainment of dry air, that forces the surface evaporation and reduces the temperature dependence, provided the surface can evaporate freely. However, the diurnal cycle over land is so strong that it is not obvious when these "equilibrium" solutions are useful. Typically even over moist surfaces, evaporation is not sufficient during the day to prevent relative humidity from falling and the LCL from rising. Furthermore, sequences of days without rain involve the integration over a series of diurnal cycles (see section 2.5)

2.3. Vegetative Controls

The physical and biological controls on vegetative resistance to evaporation are well documented [e.g. *Jarvis*, 1976; *Monteith*, 1975, 1976; *Nobel*, 1983; *Sellers et al.*, 1992]. Vegetation loses water by evaporation through open stomata as it takes up CO_2 for photosynthesis. This process is controlled by light levels and subject to other biological controls. For example, if the atmospheric relative humidity is low, some species will respond by closing stomata to restrict water loss. This is indicated schematically by the light solid feedback line in Figure 1. These processes have been included in many detailed land surface parameterizations [e.g. *Dickinson*, 1984; *Dickinson et al*, 1986; *Sellers et al.*, 1986], and are not reviewed in this paper. We shall consider the feedbacks between available soil moisture, soil temperature, vegetative resistance to evaporation, and the atmospheric BL.

2.4. Subsurface Controls on Surface Bowen Ratio

The heat and moisture budget of the soil play important physical roles in the control of the partition of the surface energy fluxes to the atmosphere. These budgets have longer "seasonal" timescales. On Figure 1, soil temperature and moisture are linked to the SRB and precipitation by the heavy dashed lines marked seasonal. Soil moisture generally has a peak in spring in the central United States and falls during the summer. Over land the link between 2-m air temperature and soil temperature is present on seasonal time scales, but it is not as tight (especially in winter and at higher latitudes) as the surface coupling over the ocean. Figure 5 shows the seasonal cycle from May to December of the 15-day mean soil temperature at 10 and 50 cm below the surface (Tsoil_10 and Tsoil_50) and the 2-m air temperature (T) for a Kansas grassland site (FIFE), and the full annual cycle for 2 boreal forest sites (from BOREAS in 1994). The FIFE curves are an average over 10 sites in a 15x15 km region from the data discussed in Betts et al. (1993). One forest site is old jack pine (OJP in Figure 2) growing in conductive sandy soils; the second, about 50km away at Thompson (TH in Figure 2), is largely spruce with a thick insulating moss layer on the surface. The differences between the three sites are striking. In the upper curves over the FIFE grassland at 39°N, the 10-cm soil temperature (short dashes) and 2-m air temperature (solid) track quite closely, while the 50-cm soil temperature (longer dashes) lags a few degrees in summer. At the other extreme at 59°N in Thompson, Manitoba, under the moss surface (covered by deep snow in winter), the soil temperature has a much smaller annual cycle than the air temperature. Indeed, at 50 cm, the seasonal range is barely ±3°C, the melt period in spring lasts nearly 2 months, and the soil is approaching the condition of permafrost. At the jack pine site, where the soil is sand covered only by lichen, the 2-m air temperature (not shown) is almost identical to the spruce site, but the seasonal range of soil temperature is larger. In winter the insulating effect of snow cover limits the seasonal fall of soil temperature.

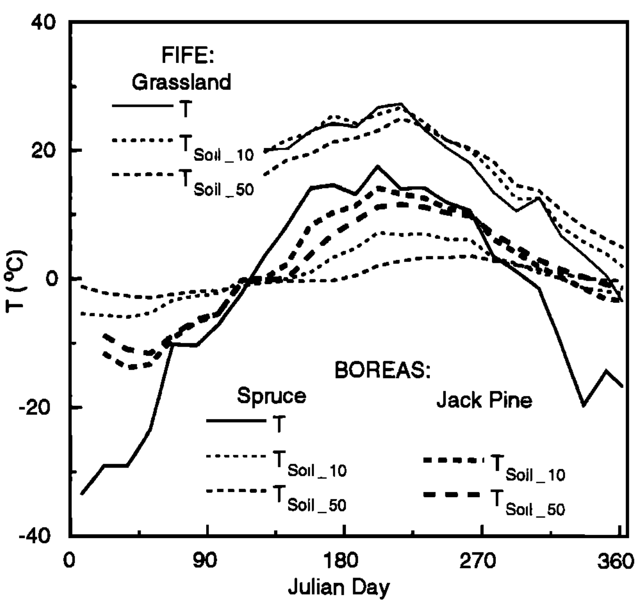

Figure 5. Seasonal cycle of soil temperature at 10 and 50 cm and air temperature, T, at 2 m for FIFE mean and two BOREAS forest sites near Thompson, Manitoba: one with sandy soil, one mostly spruce with a moss surface.

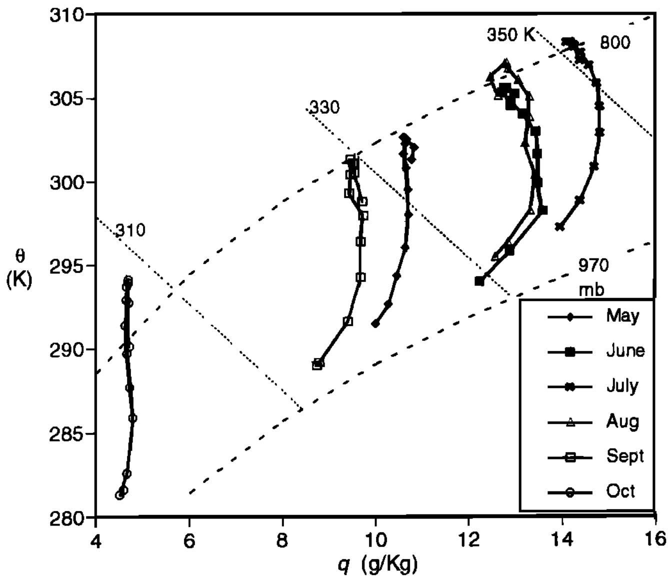

Figure 6. Daytime diurnal cycle of potential temperature (θ) and mixing ratio (q) at 2-m from 1145 to 2345 UTC for monthly dry day composites (FIFE averages for 1987).

The spring melt of the soil (and freeze in the fall) introduces a significant thermal seasonal lag into the system, which some global models do not include. In addition, there appears also to be a direct feedback between soil temperature and forest evapotranspiration in spring. It was found during BOREAS [*Sellers et al.*, 1995] that evaporation from the forest in spring stayed low until soil temperature warmed. In Figure 5, the soil temperature at 50 cm at the spruce site does not rise above freezing until around July 1 (Julian day 182), after the summer solstice. Although the boreal forest is dotted with numerous lakes, evaporation from them is also low until they warm up relative to the air in late summer and fall.

2.5. Seasonal Cycle of the Diurnal Cycle

Figure 6 shows the daytime diurnal cycle of the FIFE 2-m thermodynamic data for the predominantly sunny and dry days from May to October 1987. The axes are potential temperature (θ) and mixing ratio (q). This (θ,q) plot can be regarded as the heat and moisture budget on orthogonal axes [*Betts*, 1992]. There are 19, 21, 25, 22, 23, and 22 days in each average in the sequence from May to October. The selection criteria were near-noon Rnet above a threshold (which was 450 W m^{-2} in midsummer, falling to 300 W m^{-2} in October) and no significant daytime rainfall [*Betts and Ball*, 1995]. Here we can see both the diurnal and seasonal cycle together. The points are plotted only hourly, starting at 1145 UTC, shortly after sunrise in midsummer. The seasonal rise and fall of mean temperature and mixing ratio can be seen; July is the warmest month. October is noticeably drier, after the vegetation has died and evaporation is low. Saturation pressure lines of 970 and 800 mbar are shown dashed. The surface pressure is near 970 mbar. It can be seen that at the morning minimum temperature, the 2-m air is about 30 mbar from saturation, except in October, when it is more unsaturated. The diurnal range of mixing ratio q is relatively small in all months. There is generally a rise of q in the morning, when the BL is shallow and capped by relatively moister air from the BL of the preceding day, and a fall in the afternoon, as the growing BL entrains drier air from higher levels. May shows no afternoon fall of q, probably because of the higher soil moisture and evaporation. May and June do not reach as low afternoon saturation pressures as the later months July, August, September, and October. This means a lower mean LCL or cloud base in the spring. Probably this reflects the seasonal drying of the surface, although changes in upper air thermodynamic structure may be involved. It is clear that the afternoon maximum of θ_e is controlled mostly by the seasonal shift. The isopleths of θ_e=310, 330, 350 K are shown dotted. The rise of θ_e from morning minimum to afternoon maximum is around 14 K in all months. As we showed in Figure 5, the seasonal shift of air temperature for the FIFE site is closely linked to that of the soil temperature.

2.6. Atmospheric BL Evolution and Feedback

Over the tropical oceans the surface SH flux and weak downward entrainment of heat at cloud-base balance the radiative cooling of the subcloud layer; while the surface evaporation is transported upward in the shallow cloud layer to balance the drying effect of large-scale subsidence [e.g. *Betts*, 1975; *Betts and Ridgway*, 1989]. Episodic precipitation affects the ocean salinity, but has little direct effect on surface evaporation. In contrast, the atmospheric boundary layer (ABL) over land has a strong diurnal cycle forced by the daytime solar heating, and by the daytime surface sensible heat flux. During the daytime the ABL warms and grows rapidly as the surface potential temperature rises, while mixing ratio typically rises and then falls (see Figure 6), changing little during the day as the surface evaporation is balanced in the ABL by the downward mixing of dry air from above. During the daytime, the ABL controls that are important for the near-equilibrium conditions over the ocean (subsidence and radiative cooling), are much smaller than the deepening and heating forced by the surface SH flux. However, during the recovery of the system at night, when the surface cools radiatively and uncouples (dew may also be deposited at the surface), the atmosphere above continues to sink slowly and dry with radiative cooling. In the long-term mean, the average of these day and night processes is similar (over moist soils) to the near steady state oceanic case (see section 2.8), but this climate land cycle (corresponding to *Betts and Ridgway* [1989] has not been fully formulated. One complication over land is that, unlike the BL equilibrium over the tropics where the precipitation branch of the circulation can be partly separated [e.g. *Sarachik*, 1978; *Betts and Ridgway*, 1989], over land the precipitation, which replenishes the ground water, is an integral part of the local climate, which locally cools and moistens the surface. Another modeling complication over land is the feedback between the shallow cloud field, the SRB, evapotranspiration and the BL moisture budget [*Ek and Mahrt*, 1994; *Wetzel and Boone*, 1995]

Figure 7 shows a sequence of soundings from Thompson in Manitoba for June 10, 1994. The morning sounding at 1116 UTC is soon after sunrise, and the strong surface inversion can be seen, about 200 m deep. Above this surface inversion, a deep well-mixed BL extends to 2200 m, formed in the region the previous day. The sun is approaching its zenith for the year. It is a clear day noon, Rnet≈550 W m^{-2}, but evapotranspiration from the forest, the lakes and fens is still small, primarily because the ground (see Figure 5) and lakes are still cold. Measurements from aircraft [*MacPherson and Betts*, 1995] estimated that the mean surface BR≈1.8 at local noon. Initially after sunrise, the large SH flux warms the shallow BL rapidly, until around 1100 local time (1700 UTC), the BL deepens

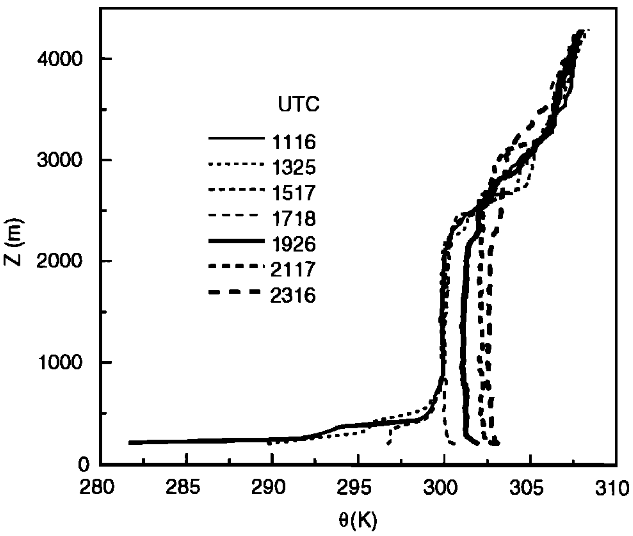

Figure 7. Sequence of 2-hourly soundings (potential temperature against height above sea level) at Thompson, Manitoba for June 10, 1994. Time is UTC.

rapidly into the preexisting deep BL. Thereafter, the reestablished deep BL warms only slowly to give an afternoon equilibrium, which is only a little warmer than the previous day. It is clear that sequences of days must be considered to understand the diurnal evolution. Note that although the afternoon 2-m air temperature, and the forest canopy, have reached 30°C (surface pressure is 983 mbar), the soil at 50 cm below the surface is still frozen at one nearby site, the spruce site in Figure 5. The low surface evaporation also had the consequence that the afternoon relative humidity at the surface fell as low as 20%. These deep warm BL's were quite common over the boreal forest in spring, a natural consequence of the large solar heating and the low evaporation. This appears to have the synoptic consequence of shifting the main summer baroclinic zone to the north of the boreal forest [*Pielke and Vidale*, 1995].

2.7. Soil Moisture, BL Entrainment and θ_e Balance

The sum of surface SH and LH fluxes are a surface source increasing θ_e (see, for example, *Betts and Ball*, [1995]). This surface θ_e flux is proportional to the *sum* of the SH+LH, and it is not affected by the Bowen ratio. It is entrainment of low θ_e air from above the BL, together with the deepening of the BL, that reduce the BL θ_e rise, and so feed back on both shallow and even more importantly on precipitating convection. Thus one of the important aspects of the BL evolution over land is how large is entrainment at BL top. The daytime BL over land is primarily thermally generated (in strong winds, shear plays a role), and thus linked to the surface virtual heat flux (which over land is usually dominated by the sensible heat flux). Hence if the surface BR is large, although the surface θ_e flux may be unchanged, the large SH flux drives more entrainment, produces a deeper BL, and the diurnal rise of θ_e is reduced. Figure 8 shows how this diurnal cycle over land depends on surface evaporation.

A total of 28 days from July and August 1987 during FIFE [*Betts and Ball*, 1995], which were affected little by precipitation or cold air advection, were composited by soil moisture (SM· measured gravimetrically in the top 10 cm). The

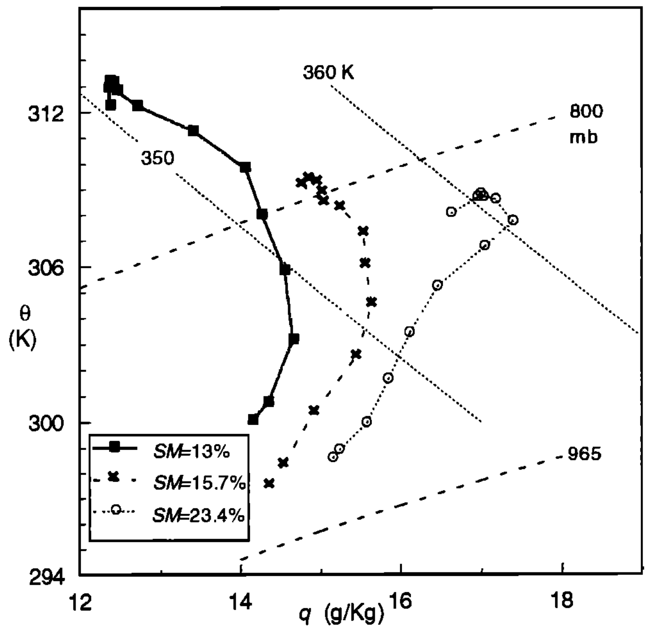

Figure 8. (θ,q) plot of surface data for selected 28 days from July and August 1987, composited by soil moisture, showing dependence of mean diurnal cycle on surface evaporation.

points are hourly values from 1115 UTC (near sunrise) to 2315 UTC. The dry soil composite (SM=13%, for which the measured mean surface BR at noon was 0.8) reaches a higher afternoon maximum θ, but at the same time a much lower q, with an afternoon $\theta_e \approx 352$ K (the θ_e isopleths are shown dotted). In contrast, the wet soil composite (SM=23.4%, for which BR at noon was ~0.4), reaches a much cooler afternoon θ maximum, but at a much wetter q value, so that the afternoon $\theta_e \approx 361$ K. Some of this shift of θ_e is associated with the shift of the entire diurnal path to higher q with higher soil moisture, but about half is the result of reduced entrainment of dry low θ_e into the BL. Over wet soils, the surface SH flux is much reduced and the BL deepens less rapidly. For all three composites, the surface available flux (Rnet-G) were nearly identical, so that the surface θ_e fluxes were similar. This local feedback between soil moisture, evaporation and afternoon θ_e equilibrium probably produces on large spatial scales a positive feedback between soil moisture evaporation and precipitation, which has been the subject of much research (see, for example *Brubaker et al.*, [1993]). The analogy over the tropical oceans is the link between BL θ_e and SST, which influences the prevalence of deep convection over warmer water [*Graham and Barnett*, 1987]. Over land, variations in soil moisture can lead to as large differences in BL θ_e as several degrees in SST. This link however remains to be explored fully. On continental scales, higher soil moisture and higher evaporation over land would lead to a higher afternoon θ_e maximum relative to the surrounding ocean and shift more of the global precipitation over the continents (see section 2.8). This feedback has been seen in global models [*Mintz*, 1984]. On the regional scale, our study of the 1993 Mississippi flood, suggested that the multiple BL's over the midwestern United States controlled the *location* of precipitation, rather than this mechanism (see section 4.3).

In the last few years, several studies of BL entrainment over land have suggested that downward mixing at BL-top is larger than expected [*Dubosclard*, 1980; *Clarke*, 1990; *Culf*, 1992; *Betts*, 1992; *Betts and Ball*, 1994, 1995]. The mixed-layer model [*Betts*, 1973; *Carson*, 1973; *Tennekes*, 1973], with a closure parameter of -0.2 relating inversion level virtual heat flux to the surface virtual heat flux, has been widely used in parametric models for two decades [see *Stull*, 1988]. The observational papers cited above suggested that the closure parameter over land may be twice as large, ≈ -0.4. The reason is still unclear, although several possibilities can be suggested. One is that the shallow cumulus field, so often present in summer, enhances the vertical transports through cloud base. In strong wind regimes, shear generated mixing plays a role. Another is that mesoscale circulations associated with topography or surface inhomogeneities [*Segal et al.*, 1988; *Avissar and Pielke*, 1989; *Avissar and Chen*, 1993] may enhance the vertical transports on the mesoscale. The diurnal evolution of the BL integrates surface fluxes and vertical transports over a range of horizontal scales of order 100 km (corresponding to 6-hours advection time over the landscape). In a global model we seek a realistic representation of the daytime diurnal cycle.

2.8. Comparison of Land and Ocean Surface Energy Balance

Another perspective on the transition from ocean to dry land is given in Table 1. This compares the *diurnally averaged* components of the surface energy balance over land for the three July-August soil moisture composites (in Figure 8) with the tropical ocean mean from *Betts and Ridgway* [1989]. The net radiation values are very similar (FIFE is summer data at 39°N in summer; the tropical average is representative of the tropics at the equinoxes), and the mean fluxes into the ground and ocean are also similar Although the surface (SH+LH) values are similar for these land and ocean cases, the surface BR show a smooth progression from dry to wet soils through to the ocean case. The mean values of T and q similarly show

Table 1. Land and Ocean Surface Energy Balance

SM, %	Rnet, Wm^{-2}	G, Wm^{-2}	SH, Wm^{-2}	LH, Wm^{-2}	BR	q, g kg^{-1}	T, °C	T_{sfc}, °C	T_{soil_10}, °C	θ_e, °K	P_{LCL}, mbar	T_{Max}, °C	θ_{eMax}, °K
13	181	20	48	114	0.42	13.8	30.2	30.7	27.7	347	152	36.8	353
15.7	189	19	37	140	0.26	15.0	27.1	27.2	25.7	348	99	33.3	355
23.4	175	13	19	153	0.12	16.0	26.4	25.4	25.2	350	79	32.3	361
Tropical ocean	177	18	9	150	0.06	16.6	26.0	26.9		347	58	26	

smooth progressions from dry land to ocean, but the mean θ_e does not. Over land, the values are marginally higher than the ocean, but show little trend. Over land and ocean, the diurnally averaged surface temperature $T_{sfc} \approx T$; over land we also show the 10-cm soil temperature. The next column is the pressure height of the LCL above the surface. This shows a smooth progression reflecting the trend of surface evaporation.

However, the diurnally averaged picture over land is of course misleading. A large diurnal cycle is imposed on these means, illustrated by the last two columns which show T_{Max} and $\theta_{e\,Max}$ for the land data sets. As shown in Figure 8, the dry land composite reaches the highest T_{Max}, but the wet composite reaches the highest $\theta_{e\,Max}$ of 361 K. This value is significantly larger than the ocean steady state value of 347 K, despite similar mean surface radiative forcing. Precipitating convection responds on short time scales to BL θ_e, and warms the deep troposphere towards a corresponding θ_e moist adiabat (typically a virtual adiabat in the lower troposphere, [*Betts*, 1986]). Consequently, the high afternoon θ_e over moist continents will preferentially force diurnally pulsed deep convection over the continents (as is seen almost daily over Amazonia).

3. Validation and Improvement of New Surface Parameterizations in Global Models

In a global model, accuracy in the surface fluxes is needed, but this is difficult to achieve over land since they are calculated from the solution of an interacting chain of parameterizations for subsurface and near-surface processes, as well as clouds, radiation and precipitation. It has only been recently that measurements from detailed field programs have been used to explore the systematic errors in these near surface parameterizations in global forecast models. Since this has produced rapid model advances, we shall review for illustration recent experience at ECMWF.

3.1. Use of FIFE 1987 Data to Identify Systematic Errors

The long time series of data from the Kansas FIFE-1987 data was used to identify systematic errors in the ECMWF model for many of the components shown in Figure 1. The details were presented by *Betts et al.* [1993], so we only summarize the results here. Different versions of the ECMWF model were at that time designated by model "cycle" numbers. The biases identified by *Betts et al.* [1993] were characteristic of model cycle 47 and earlier cycle numbers. At that time the land surface scheme was that developed by *Blondin* [1991]. We found that incoming solar radiation at the surface in the model was too large even under clear skies. Some changes to the radiative code have since reduced this bias. Subsequently, it was noticed that the model had too little cloudiness. This is being partly remedied by the introduction of a prognostic cloud scheme [*Tiedtke*, 1993; *Viterbo and Courtier*, 1995]. The unstressed vegetative resistance then in the model (model cycle 47 and earlier) was too low in comparison with the FIFE data over grassland. The BL model had very little entrainment at BL-top, because it used a downgradient diffusion scheme [*Louis*, 1979; *Louis et al.*, 1982]. Consequently, the BL was too shallow and did not represent well the diurnal cycle of temperature and moisture. The soil thermal model had serious errors. Thermal transfers to the atmosphere depended on first heating up the 7-cm-thick upper soil layer. This required a very large heat flux into the ground after sunrise (which was made worse by a time truncation problem). This introduced an error in the 24-hour average ground heat flux, and a phase lag of about 2 hours in the surface SH and LH fluxes during the daytime. The EC model (prior to cycle 48) used the first 7-cm soil layer temperature as the surface temperature (T_{sfc}). Figure 9 adapted from *Betts et al.* [1993] illustrates the effect on air temperature and surface temperature of some of the model deficiencies for a 7-day average in early October 1987. The time axis is hours after 1200 UTC (local solar noon is at 6.3 hours). The 2-m air temperature, T_K (in K), in the model is about 4 K higher than the afternoon maximum measured by an average of the FIFE stations. The model maximum is also shifted a little later in time. The observed surface radiometric temperature (labeled T_{SfcK}) exceeds T_K by 5 K, while the corresponding difference in the model is only 2 K (where the "surface" is a 7-cm-thick soil layer). After sunset, the surface and air temperature cool much more slowly in the model than observations, so that the morning minimum of temperature is again too high.

However, the systematic errors which had probably the largest impact on the model performance were in the subsurface hydrology. The model predicted the soil moisture in the top 7-cm soil layer and the second 42-cm layer. In the design [*Blondin*, 1991], it had been intended that these two layers would represent the daily and weekly timescales for the soil memory. Beneath these two predicted layers was a 42-cm "climate layer" with temperature and soil moisture taken from *Mintz and Serafini* [1992], and fixed for each month. *Betts et al.* [1993] found that this hydrology model did not work as intended. The shallow 7-cm layer dried out quickly on successive days without rain. The next predicted 42-cm layer (which has a larger capacity for moisture storage) is not replenished rapidly during rainfall. It was replenished by hydraulic diffusion with a timescale of order 10 days. Consequently, since the shallow layer dries out quickly, the soil moisture in the next layer is controlled primarily by diffusion from the (specified) climate layer at the base, which had dry values in midsummer. As a result, the model could not maintain high evaporation for more than a few days without

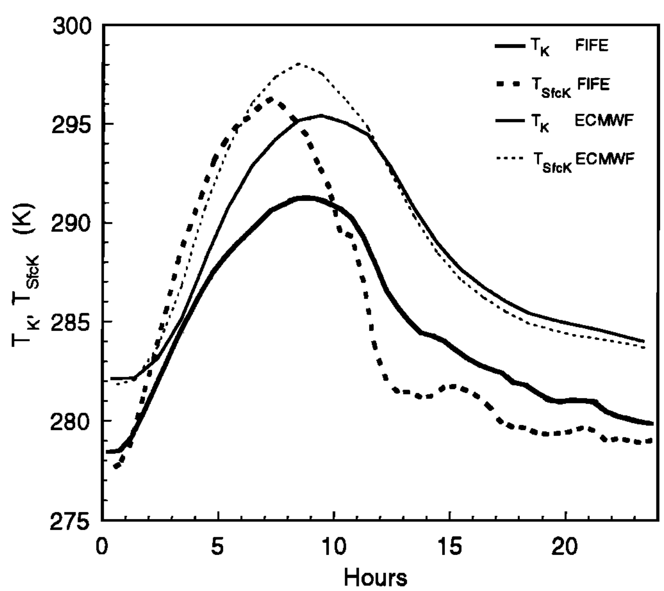

Figure 9. The 7-day October 1987 average comparing FIFE data and the second day of ECMWF forecasts (cycle 39) verifying on the same dates.. Adapted with permission of the Royal Meteorological Society from Betts et al. [1993].

rain, whereas the grassland prairie can store water for several weeks [*Kim and Verma*, 1990] This comparison of the subsurface hydrology and evaporation showed a few simple lessons. First, a mechanism is necessary to get precipitation rapidly into the ground, where it can be stored. Second, sufficient storage is needed to represent several weeks of evaporation without rain. Third, seasonal and interannual memory of soil moisture anomalies needs deep predicted reservoirs.

3.2. Development of New Land Surface and BL Submodels at ECMWF

The European Centre tested and developed new components of the land surface and BL parameterizations to correct these model errors. Most of these changes were introduced in a new model cycle 48, which became operational on August 3, 1993, and was run in parallel with the previous operational cycle 47 during July 1993 (see section 4.3). *Viterbo and Beljaars* [1995] discuss the new land surface parameterization. In its development, they used in addition to the FIFE data set field, observations from different climate regimes, Cabauw in the Netherlands and Amazon Rainforest Meteorological Experiment (ARME) in Brazil.

To summarize briefly, the biggest changes were in the soil model. The soil model now has four predicted layers, plus a predicted skin temperature, and a thin surface water layer representing interception of precipitation, or the collection of dew. The bottom boundary conditions are zero heat flux and free drainage. The four soil layers have depths of 7, 21, 72, and 189 cm, with a root zone in the first three layers. The deepest layer acts as a reservoir and a memory for the longer time scales (of order a year). The formulation of the soil hydraulic properties were revised to increase the downward infiltration of precipitation from a saturated surface. The introduction of a skin temperature, which is calculated from flux equilibrium at the surface, reduces the errors in the ground heat flux, and the phase errors in the SH and LH fluxes discussed in the previous section. A smaller roughness length for heat (and moisture) than momentum was introduced based on a FIFE estimate [*Betts and Beljaars*, 1993] as well as other work. This increases T_{sfc} - T. Improvements in the prediction of the surface skin temperature improve the accuracy of the surface long-wave emission. The BL parameterization was revised (Beljaars and Betts, 1993) to represent entrainment at BL top by introducing diffusion coefficients specified according to a similarity profile (a version of the scheme of *Troen and Mahrt* [1986]. The model still has a fixed vegetation fraction at each grid point. The unstressed vegetative resistance, which is the same at all gridpoints, was increased in the new model to match the FIFE grassland data. Single-column integrations of the new and old model were compared with data sets from FIFE, ARME, and Cabauw in the Netherlands [*Viterbo and Beljaars*, 1995]. Single-column tests are a powerful means to isolate deficiencies in the land surface parameterization from other model deficiencies.

4. Impact of Soil Moisture on Precipitation Forecasts

The introduction of four predicted layers for soil moisture had a large impact on the precipitation forecasts of the ECMWF model on a variety of scales. In agreement with the climate model studies reviewed by *Garratt* [1993], reducing soil moisture over the continents reduces continental precipitation on long timescales. This is consistent with sections 2.7 and 2.8, where we discussed the link between dry soil, low evaporation, more boundary layer entrainment and a lower afternoon θ_e maximum. If evaporation is reduced on a continental scale, this could reduce the afternoon θ_e equilibrium over the continent relative to the ocean, reduce tropospheric heating by deep convection, reduce continental-scale convergence, and so have a positive feedback in reducing the mean continental precipitation. This appears to happen in the model. One consequence of this, however, is that initializing the global fields of soil moisture for the new model cycle 48 presented difficulties.

4.1. Global Initialization of Soil Moisture Fields

Unlike SST, maps of soil moisture and temperature are not available to initialize a global forecast model. During data assimilation, the model precipitation field and surface fields can be used to drive the subsurface budgets, but the long memory of soil moisture would require long periods of (costly) data assimilation. In addition, it was not known whether the model would drift to its own climate state influenced for example by known model errors in the surface radiation budget. Subsequently, this was found to be the case. Instead, the new model cycle 48 was run for 4 years at a spectral resolution of T-63 in an attempt to derive a model soil moisture 'climate' by averaging this 4-year run. However, it was clear that the summer continental precipitation over say the Uuited States was too low and that the model had drifted to a dry soil climate. This drift of the model in climate mode appeared to be a result of an excess of net radiation at the surface associated in part with too little cloudiness in the model [*Viterbo and Courtier*, 1995] and too little short-wave absorption [*Betts et al.*, 1993]. This overestimation in models of incoming short-wave radiation at the surface appears to be a widespread error [*Cess et al.*, 1995].

A second study using 120-day T-63 simulations for the summer of 1992, showed the sensitivity of the summer precipitation over the Uuited States to the specification of initial soil moisture on May 1. A positive feedback was apparent between continental-scale soil moisture and precipitation, as has been seen in climate models [*Garratt*, 1993]. Starting with initially wet soils (corresponding to unstressed evapotranspiration) on May 1, 1992, gave roughly double the continental-scale precipitation for the 3 month (JJA) period than the corresponding simulation starting with low soil moisture (for which the vegetation was stressed). In both simulations the mean soil moisture dried out with the seasonal cycle, but because the moist soil initial condition produced more precipitation, the memory of the initial condition was not lost even in a 120-day forecast. This clearly is an important issue for the initialization of a global (or regional) forecast model. Over the oceans, solving a coupled ocean model can be avoided for medium-range forecasting by specifying a measured SST as a surface boundary condition, although this is not adequate for seasonal forecasting. Over land, it appeared that the present surface boundary condition could only be determined by long periods of data assimilation and even for this, a model needs a good surface radiation budget (which means in practice realistic cloud fields). In the summer of 1993, this issue was avoided by starting the new operational cycle 48 on July 2 with soil moisture in vegetated areas at field capacity (it had been a wet spring over much of the northern hemisphere), and running a month of data assimilation before operational implementation on August 3. This by chance was the month of the major flooding of the Mississippi, so it allowed us to look at parallel forecasts with two model cycles with very different land surface schemes (see section 4.3). In addition, we looked at 30-day forecasts for the month of July with the new model and different initial soil moistures (see section 4.2). The issue of soil moisture initialization was not really resolved however. The data assimilation continued with the new model cycle over the winter of 1993/1994. However, by June 1994, it was clear that soil moisture, and the model surface parameters, had drifted towards too dry and warm a state. Again this appeared to result from too much incoming radiation at the surface because of too little cloudiness. Objective forecast scores in June 1994 were poor, and at the beginning of July the soil moisture was reinitialized at field capacity, which improved the model performance. Simultaneously, experiments with the nudging of soil moisture, based on 2-m humidity errors, showed a large positive impact on surface errors and forecast skill (see section 4.4).

4.2. Sensitivity of 30-day Integrations for July 1993 to Initial Soil Moisture

Two ensembles of three 30-day integrations using cycle 48 (Cy48) at T106 resolution starting from the Cy48 analysis for July 1, 2 and 3 were compared [*Betts et al.*, 1994; *Beljaars et al.*, 1995] The only difference was the initial soil moisture. One "wet soil" ensemble was initialized at the soil field capacity, the other "dry soil" ensemble with only 25% of the "available" soil moisture. Available soil moisture is the difference between field capacity, and the soil moisture corresponding to the permanent wilting point of the vegetation, when no more moisture can be extracted from the soil (see *Viterbo and Beljaars* [1995] for details of the vegetation model). Figure 10 shows the *difference* in the mean July precipitation in milimeters per day between the wet and dry soil ensembles. The higher initial soil moisture has increased precipitation over most of the United States, except the southeast. Perhaps remarkably, Figure 10 has a considerable resemblance to Figures 11a and 11b, the observed July precipitation field and the anomaly field (a deviation from the 30-year mean). The band of large precipitation increase across the central US near 41° N in Figure 10 (the shaded area is a precipitation increase greater than 4 mm/day or 124 mm/month) is a little north of the observed precipitation peak (the Kansas-Nebraska border in Figure 11a is at 40°N), which caused the catastrophic Mississippi flood Nonetheless the resemblance is remarkable, considering that the initial soil moisture fields in the model were assumed fields. It had been wet the previous fall and winter across the central United States with above normal precipitation in Spring 1994 [*Kunkel et al.*, 1994]. Flooding had already started in June, and near-saturated soils existed across an extensive area of the mid-West [*Junker et al.*, 1995]. Figure 10 suggests that the initial high values of soil moisture coupled to a long-term feedback, contributed to the July flood, in conjunction with the persistent large-scale atmospheric pattern [*Kunkel et al.*, 1994].

4.3. Short-Term Forecasts From Parallel Runs of Cycle 47 and 48

Since parallel runs of the data assimilation and 10-day forecast system with two model cycles were available at ECMWF from July 2 to 22, 1993, it was possible to compare the short-term precipitation forecasts with observations for the critical period of heavy rain over the upper Mississippi. Historically, summer precipitation forecasts have not been accurate quantitatively beyond 48 hrs. This was true for the operational model cycle 47 (Cy47) which, as discussed in 3.1, had a land surface scheme with little memory of soil moisture beyond a day or two. In contrast, the new model Cy48 with four prognostic soil layers (which was to become the operational model on August 3), showed skill in predicting

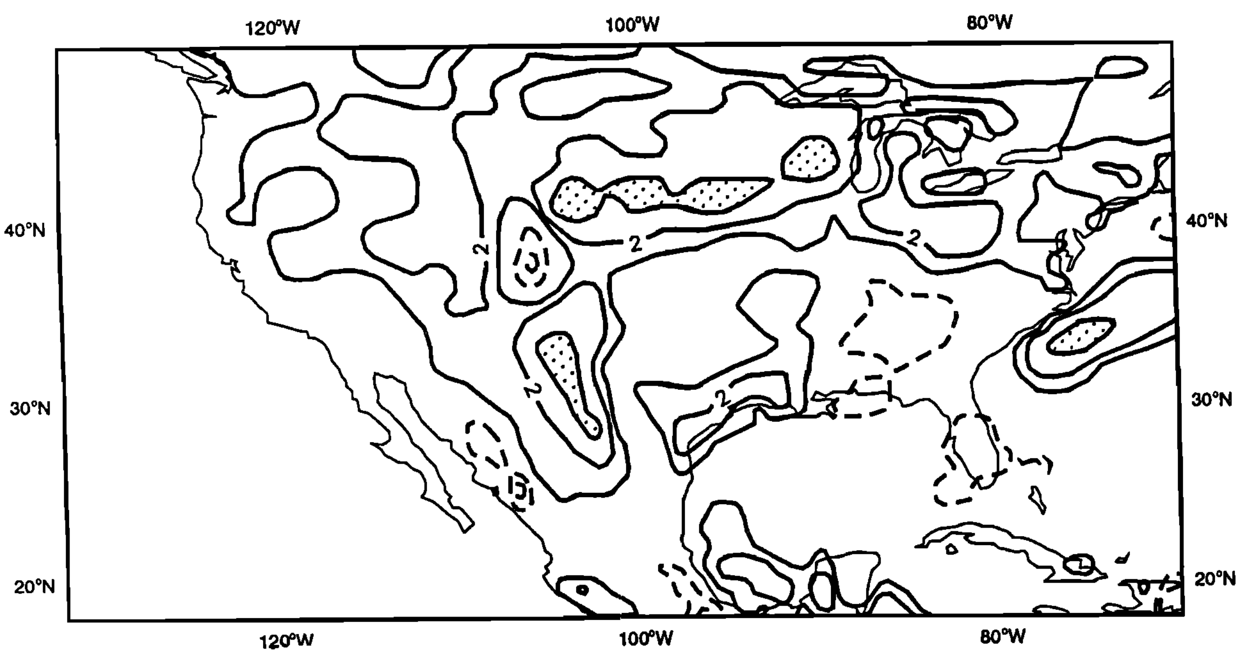

Figure 10. Difference in precipitation forecast by Cy48, starting with wet and dry initial soil moisture, averaged over an ensemble of three 30-day forecasts at T106L31 resolution starting from July 1, 2, and 3, 1993. Shaded area is increase greater than 4 mm/day, dashed contours indicate reduced precipitation. Adapted with permission of the American Meteorological Society from Beljaars et al. [1995].

precipitation at much longer forecast times. Figure 12 [from *Beljaars et al.*, 1995] shows a comparison of the mean 48-72 hour forecast precipitation verifying between July 9 and July 25 over the United States from Cy47 and Cy48, together with station observations in millimeters per day. The difference is striking. Whereas Cy48 (lower panel B) gives an excellent forecast of the precipitation in the flood region, Cy47 (upper panel A) forecasts a precipitation maximum well to the north. *Beljaars et al.* [1995] discuss in detail the mechanism for this improvement in forecast accuracy. It involves yet another BL mechanism distinct from the local diurnal cycle issue, discussed in section 2.8, and the continental-scale feedback between precipitation and surface evaporation discussed in section 4.1. The location of the heavy precipitation over Kansas involves the breakdown of a capping inversion formed by an overlying pre-existing BL from the Mexican plateau to the southwest, which overlies the cool moist BL originating in the Gulf of Mexico. This characteristic storm environment has been studied for many years [e.g. *Carlson and Ludlam*, 1968; *Carlson et al.*, 1983]. Numerical simulations have also shown that evaporation controlled by soil moisture plays an important role in the formation and breakdown of this double BL structure [*Lanicci et al.*, 1987]. In the ECMWF July 1993 forecasts, the upper capping mixed layer in the Cy47 model was too warm and dry, due to too little surface evaporation upstream the previous day. Consequently the low level flow from the Gulf did not break through this capping inversion until much further north. In contrast, the new model Cy48 reproduced the double BL structure more realistically, and as the low level Gulf flow curved northeastward over Kansas, the capping inversion was sufficiently weak to permit deep convection to develop in the region observed. Thus it is clear that the accurate prediction of summer precipitation in this region requires the accurate prediction of multiple BL's over a wide region and several days. In this way the land surface boundary condition over a wide area interacts with the large-scale flow to control the location of major precipitation systems.

4.4. Recent improvements in forecast skill over land from Nudging Soil Moisture, and a New Prognostic Cloud Scheme

The success of these precipitation forecasts for the extreme flood event of July 1993 emphasized the more general importance of memory in the land surface boundary condition. However, soil moisture initialization remained a problem. The new model Cy48 with predictive soil moisture was integrated in the data assimilation cycle through to the spring of 1994. By May-June 1994, it was clear that the soil moisture was drying

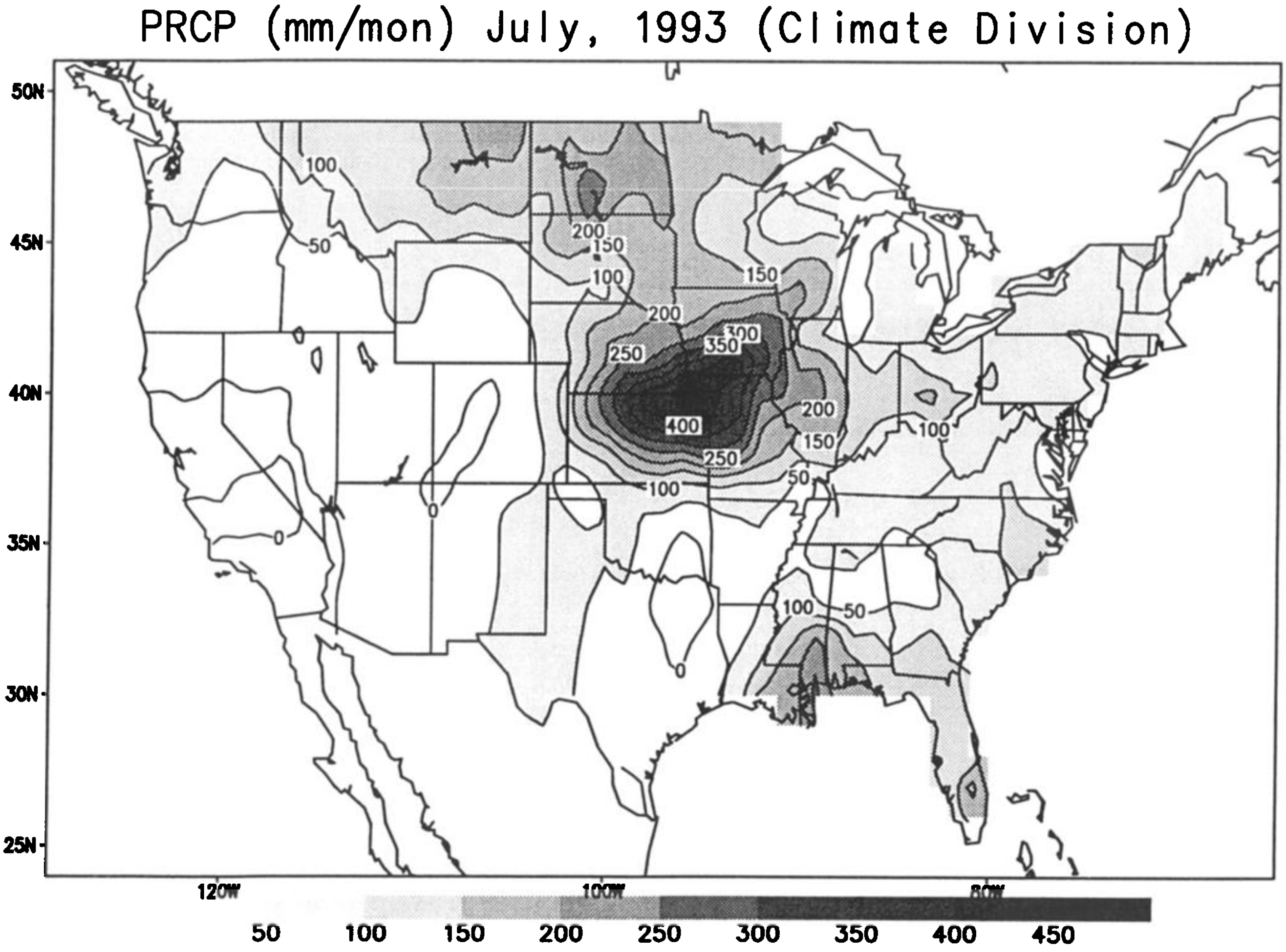

Figure 11. (**a**) Total precipitation for July 1993 over the United States. Contours are in millimeters per month. (**b**) Deviation of July 1993 precipitation from 30-yr climatology (1961-1990). Figures kindly supplied by Jin Huang, NMC Climate Analysis Center.

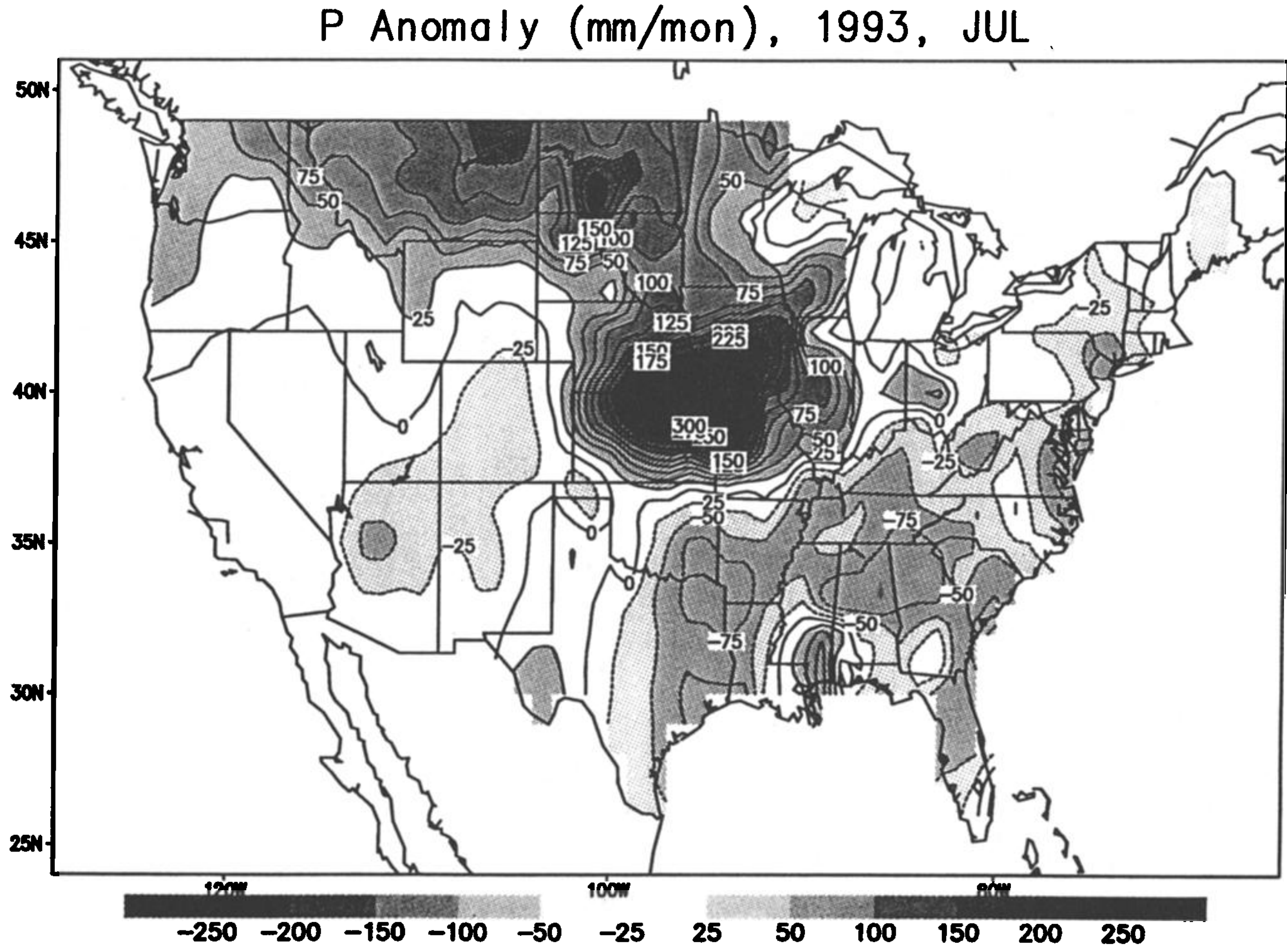

Figure 11. (continued)

out. Surface air temperature errors were increasingly positive, and in comparison with other models, such as the German Weather Service (constrained by climatological soil moisture), forecast skill was deteriorating [*Viterbo and Courtier*, 1995]. The temporary solution was to reinitialize the soil moisture at field capacity at the beginning of July 1994 (as was done to start this land surface scheme in July 1993). This removed most of the model warm bias at the surface. Simultaneously, data assimilation experiments were carried out for June 1-20 1994, with nudging of soil moisture based on the 2-m humidity errors [*Viterbo and Courtier*, 1995]. This follows, in a simplified way, the general suggestions of *Mahfouf* [1991], that near surface parameters can be used to initialize soil moisture. This nudging scheme was implemented operationally in December 1994. In the ECMWF model, the downward drift of soil moisture appears to be linked to excess incoming solar radiation primarily caused by under prediction of clouds. While this cloud and radiation error remains, nudging in essence supplies soil moisture to maintain evaporation in the face of excessive net radiation at the surface. On the basis of the discussion in 2.8, this may bias BL θ_e toward higher values. Fortunately, a new prognostic cloud-scheme, which had been under development for some time [*Tiedtke*, 1993], was implemented in spring 1995. This prognostic cloud scheme has significantly reduced the cloud radiation error over land.

Figure 13 illustrates the large reduction in forecast errors over land that have resulted from these two model changes. The upper panel shows the growth with forecast day of the bias in the mean height at 200 hPa over North America, and the lower panel the growth of root mean square error of the 200 hPa height. The dotted line with the fastest growth of the mean bias is the average of the 20 operational forecasts for June 1-20, 1994. The positive mean bias means that the troposphere over North America as too warm, and the likely cause here is the excess of net radiation at the surface. The dashed lines are for the same 20 forecasts run from an analyses which included soil moisture nudging in the assimilation cycle. We see a significant reduction in the growth of the mean bias and in the RMS error in the important forecast time period of 3-7 days. In this comparison the forecast models are the same.

The solid curves with the small negative bias in the upper panel and slower error growth in the lower panel came from using the current (April 1995) operational model (which includes a prognostic cloud scheme) for both the assimilation cycle and the June 1-20, 1994 forecasts. This model no longer appears to have a radiation bias at the surface over land due to underestimation of cloud. The mean temperature bias in the model is therefore much improved (upper panel). So is the forecast skill in the medium range (lower panel) although this may be partly due to the improved formulation of the impact of orography. For a global model these are significant improvements. They suggest that an improved surface boundary condition can have a large impact on forecast skill over land in the northern hemisphere. We have shown 200 hPa

A) Cy47

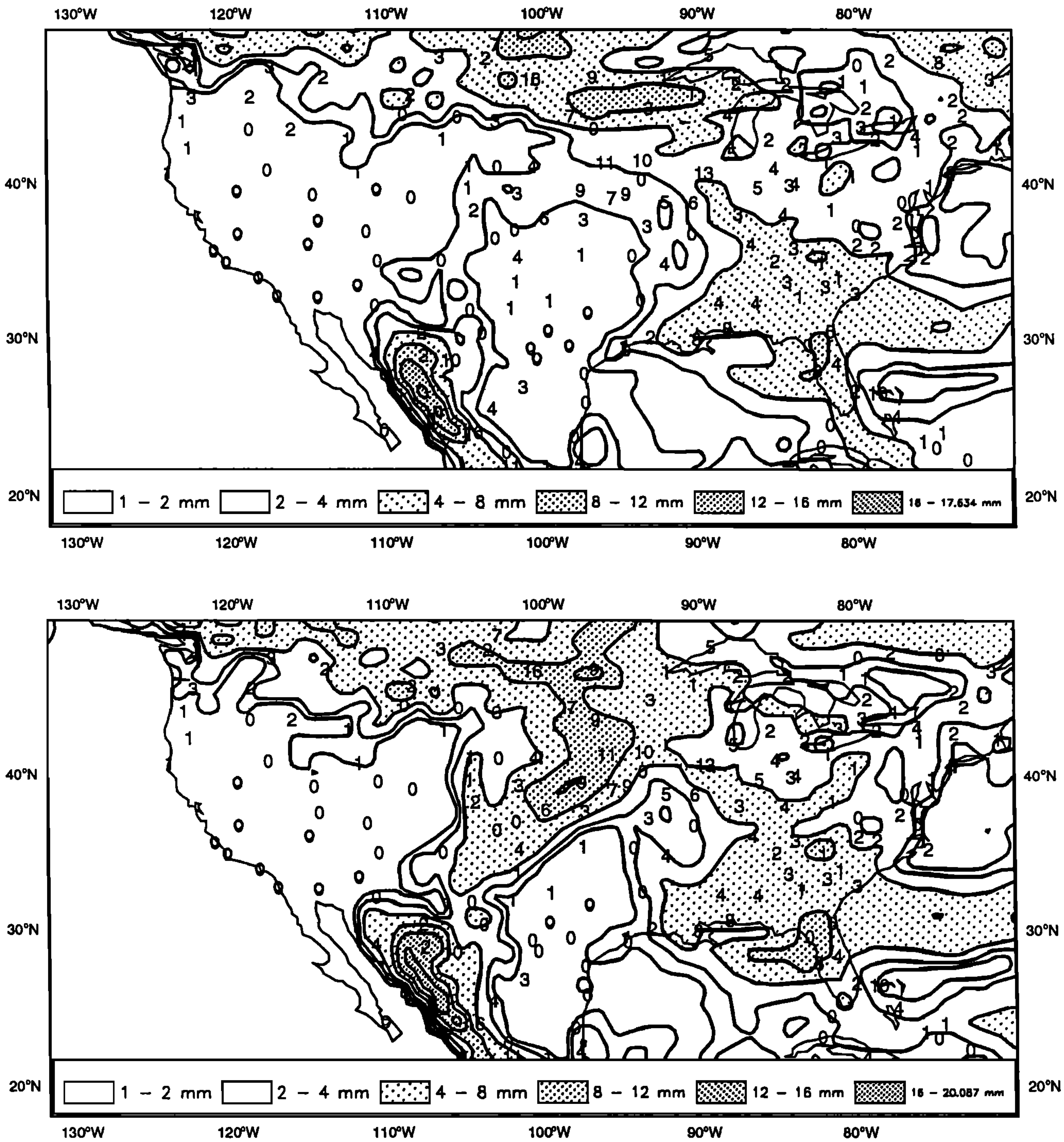

B) Cy48

Figure 12. Mean forecast precipitation for all 48- to 72-hour forecasts verifying between July 9 and 25, 1993 for (a) Cy47 (upper) and (b) Cy48 (lower panel). Contours are at 1, 2, 4, 8 mm/d; printed numbers are station observations in millimeters per day. Reproduced with permission of the American Meteorological Society from Beljaars et al. [1995].

over North America (where the improvement was largest), since this is the region of importance to GCIP, but large improvements were also seen in the 500 hPa height and in the surface errors in the northern hemisphere, as well as improvements in the model hydrologic cycle over land.

5. Conclusions

This review has addressed the land surface-atmosphere interaction from both an observational perspective illustrated by data from the FIFE and BOREAS field programs, and a

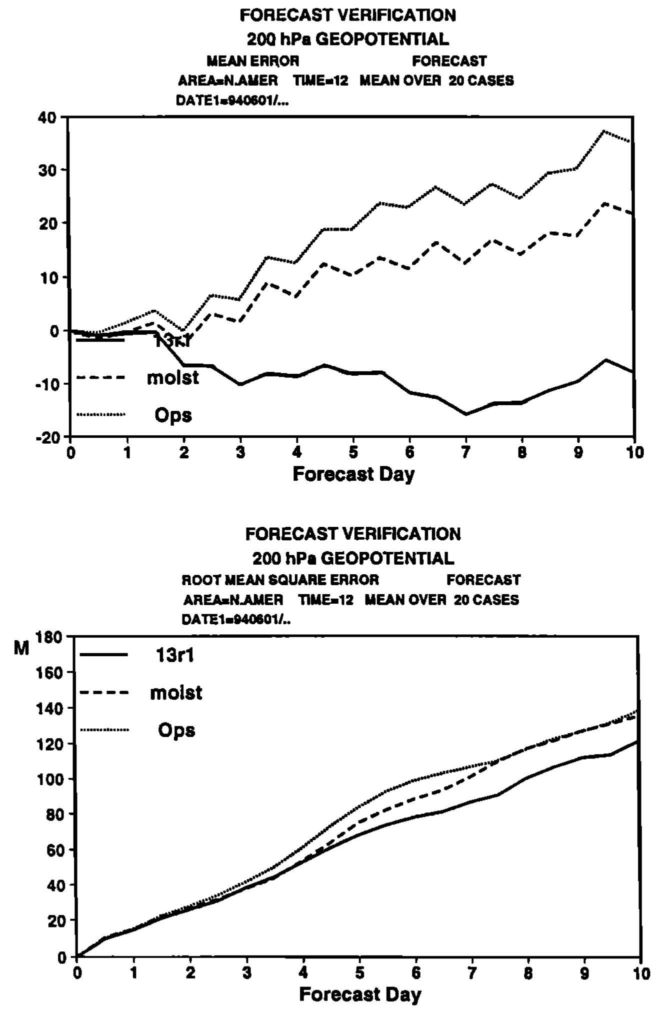

Figure 13. Mean bias error and root mean square error for 200 hPa height over North America for three sets of 20 10-day T-213 forecasts for June 1-20, 1994. The dotted control is the operational model at that time, the dashed curves ("moist") are with the addition of nudging of soil moisture in the assimilation cycle, and the solid curves (cycle "13r1") are using the current operational model cycle (May 1995), which includes prognostic clouds, for both data assimilation and forecasts.

modeling perspective illustrated by recent experience in developing the land surface, boundary layer (BL), and cloud schemes at ECMWF. Field programs have played a major role in understanding the feedbacks between the land surface and the atmosphere locally on diurnal and seasonal scales. The long time series of data from the FIFE experiment gave quantitative information on the coupling of soil moisture, precipitation, vegetation, the surface energy budget and the atmospheric BL. This has led to a clearer understanding of the local feedback between the surface energy budget and the surface Bowen ratio and BL entrainment, which brings down low θ_e air. This data set (and others) suggested that BL-top entrainment over land may be larger than anticipated. Together the fluxes from the surface and through the top of the mixed layer control the diurnal evolution of the mixed layer θ, q, θ_e, and saturation pressure, which in turn directly influence the formation of clouds and precipitation. The recent data set from BOREAS is giving insight into the tighter controls on evaporation over the northern boreal forest, which feed back on the BL evolution, giving deep, warm, dry BL's in Spring when the land surface is still cold.

Representative long-term local data sets can play an invaluable role when compared with long time series from collocated gridpoints of a numerical forecast model. Major improvements in the ECMWF land surface and BL schemes were prompted by such a comparison with the FIFE data set [*Betts et al.*, 1993], and then validated against this and other datasets from different climatic regimes. It may seem remarkable that data from the 15 x 15 km domain of FIFE could readily detect systematic errors in a complex global model with horizontal resolution of order 100 km. There are several reasons. Over the dense U.S. network, the forecast model has sufficient upper air data to describe the upper level atmospheric flow, although its formulation of near-surface processes depend largely on the model parameterizations. The 1987 FIFE data (after editing and averaging) is probably representative of larger scales than 15 km, because of the integrating effect of the ABL over the diurnal cycle. It proved relatively straightforward to identify systematic errors in the model formulation of near-surface processes by looking at the diurnal cycle of groups of days as surface evaporation changed through different seasons.

We have then traced the development and implementation of changes in the ECMWF model, and the large impact they had on model forecast skill, in particular for the period of the July 1993 Mississippi flood. Seasonal forecasting has paid a great deal of attention to the long-term memory of the climate system in the sea surface temperatures. With the development of forecast models with long-term memory in the land surface soil moisture and temperature, it is clear that improvements in predicting the summer climate over the continents may be possible. We have used the ECMWF experience as illustration. Similar work is in progress at the National Meteorological Center using similar data sets to improve both the regional model and the global medium-range forecast model. We anticipate that the data collection for GEWEX will accelerate the improvement of land surface schemes in both forecast and climate models, until the surface boundary condition over land is as well formulated as that over the ocean. However it is also clear that GEWEX will have to pay more attention to the observation and modeling of the cloud fields. The recent operational implementation of a prognostic cloud scheme [*Tiedtke*, 1993] in the ECMWF model has confirmed that the fundamental role that clouds play in the surface radiation budget feeds back on forecast skill over land within a few days.

It appears that there are several different feedbacks between the surface, the BL processes, clouds and precipitation on different scales. On the local diurnal scale, the afternoon θ_e balance is controlled by surface evaporation, which has a negative feedback on the BL-top entrainment of low θ_e air. On the regional scale, the spatial distribution of major precipitation systems involves also the accurate prediction of the double BL structure characteristic of the mid-Western United States. Here the upper BL was formed on a previous day and advected as a capping BL over the low level flow from the Gulf of Mexico. On the monthly to seasonal timescale there is a positive feedback between soil moisture, surface evaporation and precipitation on continental scales. The soil moisture (in conjunction with soil temperature) provides a long-term memory in the surface boundary condition as does SST over the oceans. On timescales beyond a few days, however, the coupling between the cloud fields, the surface radiation budget, soil moisture and surface evaporation must all be modeled with some precision.

Acknowledgments. Field experiments and global forecast models are true collaborative efforts at the heart of atmospheric science. We acknowledge all those who contributed to this research. NSF under grant ATM 95-05018, NASA under contract NAS5-32356, and NOAA under grant NA56GP0380 have all supported this research

References

Atlas, R., N Wolfson, and J. Terry, The effect of SST and soil moisture anomalies on GLA model simulations of the 1988 U.S. summer drought, *J. Clim., 6*, 2034-2048, 1993.

Avissar, R , and F Chen, Development and analysis of prognostic equations for mesoscale kinetic energy and mesoscale (subgrid-scale) fluxes for large-scale atmospheric models, *J. Atmos. Sci., 50*, 3751-3774, 1993.

Avissar, R., and R.A. Pielke, A parameterization of heterogeneous land-surface for atmospheric numerical models and its impact on regional meteorology. *Mon. Weather. Rev., 114*, 2113-2136, 1989.

Beljaars, A.C.M., and A.K. Betts, Validation of the boundary layer scheme in the ECMWF model, in *ECMWF Seminar Proceedings 7-11 September 1992, Validation of models over Europe, vol II.* pp. 159-195, Eur. Cent. For Medium Range Weather Forecasts, Reading, England, 1993.

Beljaars, A.C.M., P. Viterbo, M.J. Miller, and A. K. Betts, The anomalous rainfall over the USA during July 1993: Sensitivity to land surface parameterization, Mon. Weather. Rev., in press, 1995.

Benjamin, S.G., and T.N. Carlson, Some effects of surface heating and topography on the regional severe storm environment, I, Three-dimensional simulations, *Mon. Weather. Rev., 114*, 307-329, 1986.

Betts, A. K., Non-precipitation cumulus convection and its parameterization, *Q. J. R. Meteorol. Soc., 99*, 178-196, 1973.

Betts, A. K., Parametric interpretation of trade-wind cumulus budget studies, *J. Atmos. Sci., 32*, 1934-1945, 1975.

Betts, A. K., A new convective adjustment scheme, I, Observational and theoretical basis, *Q. J. R. Meteorol. Soc., 112*, 677-692, 1986.

Betts, A.K. FIFE atmospheric boundary layer budget methods, *J. Geophys. Res., 97*,18,523-18,531, 1992.

Betts, A.K., Relation between equilibrium evaporation and the saturation pressure budget. *Boundary Layer Meteorol., 71*, 235-245, 1994.

Betts, A.K., and J. Bartlo, The density temperature and the dry and wet virtual adiabats. *Mon. Wea. Rev., 119*, 169-175, 1991.

Betts, A.K. and A. Beljaars, Estimation of effective roughness length for heat and momentum from FIFE data, *Atmos. Res. 30*, 251-261, 1993.

Betts, A.K. and W. L. Ridgway, Climatic equilibrium of the atmospheric convective boundary layer over a tropical ocean. *J. Atmos. Sci., 46*, 2621-2641, 1989.

Betts, A.K., J.H. Ball, and A.C.M. Beljaars, Comparison between the land surface response of the European Centre model and the FIFE-1987 data. *Q. J. R. Meteorol. Soc., 119*, 975-1001, 1993.

Betts, A.K., and J.H. Ball, The FIFE surface diurnal cycle climate, *J. Geophys. Res.*, in press, 1995.

Betts, A.K. and J.H. Ball, Budget analysis of FIFE-1987 sonde data, *J. Geophys. Res., 99*, 3655-3666, 1994.

Betts, A.K., J.H. Ball, A.C.M. Beljaars, M.J. Miller, and P. Viterbo, Coupling between land-surface boundary-layer parameterizations and rainfall on local and regional scales: Lessons from the wet summer of 1993, in *Fifth Conference on Global Change Studies*, pp.174-181, Am. Meteorol. Soc., Boston, Mass., 1994.

Blondin, C., Parameterization of land-surface processes in numerical weather prediction, in *Land surface evaporation - Measurement and parameterization*, edited by T. J. Schmugge and J. C. Andre, pp. 31-54, Springer-Verlag, New York, 1991.

Brubaker, K.L., D. Entekhabi, and P.S. Eagleson, Estimation of continental precipitation recycling. *J. Clim., 6*, 1077-1089, 1993.

Brutsaert, W., Catchment -scale evaporation and the atmospheric boundary layer, *Water Resour. Res., 22*, 39-45, 1976.

Carlson T.N., and F.H. Ludlam, Conditions for the occurrence of severe local storms, *Tellus, 20*, 203-226, 1968.

Carlson, T N., S.G. Benjamin, G.S. Forbes, and Y-F. Li, Elevated mixed layers in the regional severe storm environment: conceptual model and case studies, *Mon. Weather. Rev., 111*, 1453-1473, 1983.

Carson, D.J., The development of a dry inversion-capped convectively unstable boundary layer, *Q. J. R. Meteorol. Soc., 99*, 450-467, 1973.

Cess, R.D., et al, Absorption of solar radiation by clouds: Observations versus models, *Science*, 267, 496-499, 1995.

Charney, J., W.J. Quirk, S-H. Chow, and J. Kornfield, A comparative study of the effects of Albedo change on drought in semi-arid regions. *J. Atmos. Sci., 34*, 1315-1351, 1977.

Clarke, R. H. , Modeling mixed layer growth in the Koorin experiment, *Aust. Meterol. Mag., 38*, 227-234, 1990.

Collatz, G.J., J.T. Ball, C. Grivet, and J.A. Berry, Physiological and environmental regulation of stomatal conductance, photosynthesis and transpiration: A model that includes a laminar boundary layer, *Agric. For. Meteorol., 54*, 107-136, 1991.

Culf, A. D., An application of simple models to Sahelian convective boundary layer growth. *Boundary Layer Meteorol. 58*, 1-18, 1992.

Culf, A.D., Equilibrium evaporation beneath a growing convective boundary layer, *Boundary Layer Meteorol., 70*, 37-49, 1994.

De Bruin, H.A.R., A model for the Priestley-Taylor Parameter α, *J. Clim. Appl. Meteorol., 22*, 572-578, 1983.

Dickinson, R.E., Modeling evapotranspiration for three dimensional global climate models, in *Climate Processes and Climate Sensitivity, Geophys. Monogr. Sev., vol. 29*, edited by J. E. Harrison and T. Takahashi, pp. 58-72, AGU, Washington, D. C., 1984.

Dickinson, R E., and A. Henderson-Sellers, Modeling tropical deforestation: A study of GCM land-surface parameterizations, *Q. J. R. Meteorol. Soc., 114*, 439-462, 1988.

Dickinson, R.E., A. Henderson-Sellers, P.J., Kennedy, and M.F. Wilson, Biosphere-atmosphere scheme (BATS) for the NCAR community climate model, *Tech. Note NCAR/TN-275+STR*, 69 pp., Natl Cent. For Atmos. Res., Boulder, Colo., 1986.

Duboscl ard, G , A comparison between observed and predicted values for the entrainment coefficient in the planetary boundary layer. *Boundary Layer Meteorol., 18*, 473-483, 1980.

Ek, M., and L. Mahrt, Daytime evolution of relative humidity at the boundary layer top, *Am. Meteorol. Soc.,122*, 2709-2721, 1994.

Garratt, J.R. Sensitivity of climate simulations to land-surface an atmospheric boundary-layer treatments- A review, *J. Clim., 6*, 419-449, 1993.

Garratt, J.R., P.B. Koummel, and E.A. Kowalczyk, The surface energy balance on local and regional scales–A comparison of general circulation models with observations. *J. Clim., 6*, 1040-1104, 1993.

Graham, N.E., and T.P. Burnett, Sea surface temperature surface wind divergence, and convection over the tropical oceans, *Science, 238*, 657-659, 1987.

Henning, D., Atlas of the surface heat balance of the continents, in *Gebrueder Borntraeger, vol. 402*, Berlin, Germany, 1989.

Holtslag, A.A.M., and B.A. Boville, Local versus nonlocal boundary-layer diffusion in a global climate model, *J. Clim., 6*, 1825-1842, 1993.

Jarvis, P.G., The interpretation of the variations in leaf water potential and stomatal conductance found in canopies in the field, *Philos. Trans. R. Soc. London Ser. B, 278*, 593-610, 1976.

Jarvis, P.G., and K.G. McNaughton, Stomatal control of transpiration; scaling up from leaf to region, *Adv. Ecol. Res., 15*, 1-49, 1986.

Junker, N.W., R.S. Schneider and R.A. Scofield, The Meteorological conditions associated with the great Midwest flood of 1993, paper presented at Conference on Hydrology, *Am. Meteorol. Soc.*, Dallas, Tex., Jan. 15-20, 1995.

Kanemasu, E.T., et al., Surface flux measurements in FIFE: An overview, *J. Geophys. Res., 97*, 18,547-18,555, 1992.

Kim, J., and S.B. Verma, Components of surface energy balance in a temperate grassland ecosystem. *Boundary Layer Meteorol., 51*, 401-417, 1990.

Kunkel, K.E., S.A. Changnon, and J.R. Angel, Climate aspects of the Mississippi river basin flood, *Bull. Am. Meteorol. Soc., 75*, 811-822, 1994.

Lanicci, J.M., T.N. Carlson, and T.T. Warner, Sensitivity of the great plains severe-storm environment to soil-moisture distribution, *Mon. Weather. Rev., 115*, 2660-2673, 1987.

Lean, J., and P R. Rowntree, A GCM simulation of the impact of Amazonian deforestation on climate using an improved canopy representation, *Q. J. R. Meteorol. Soc., 119*, 509-530, 1993.

Louis, J.F., A parametric model of vertical eddy fluxes in the atmosphere, *Boundary Layer Meteorol., 17*, 187-202, 1979.

Louis, J.F., M. Tiedtke, and J.F. Geleyn, A short history of the operational PBL-parameterization at ECMWF, paper presented at Workshop on Boundary Layer Parameterization, Eur. Cent. for Medium Range Weather Forecasts, Reading, England, 1982.

McNaughton, K.G., Evaporation and advection, I: Evaporation from extensive homogeneous surfaces, *Q. J. R. Meteorol. Soc., 102*, 181-191, 1976.

McNaughton, K.G. and P.G. Jarvis, Predicting effects of vegetation changes on transpiration and evaporation. In *Water Deficits and Plant Growth, Vol. VII, edited by T. T. Kozlowski*, pp. 1-47, Academic,San Diego, Calif., 1983.

McNaughton, K.G., and T.W. Spriggs, A mixed layer model for regional evaporation, *Boundary Layer Meteorol., 34*, 243-262, 1986.

MacPherson, J.I. and A.K. Betts, Aircraft encounters with strong coherent vortices over the Boreal forest, *11th AMS Symposium, Boundary Layers and Turbulence*, pp. 424-427, Am. Meteorol. Soc., Boston, Mass., 1995.

Mahfouf, J.F., Analysis of soil moisture from near-surface parameters: A feasibility study, *J. Appl. Meteorol., 30*, 1534-1547, 1991.

Milly, P.C.D., and K.A. Dunne, Sensitivity of the global water cycle to the water-holding capacity of land, *J. Clim., 7*, 506-526, 1994.

Mintz, Y., The sensitivity of numerically simulated climates to land-surface boundary conditions, in *Global Climate*, edited by J. H. Houghton, pp. 79-105, Cambridge University Press, Cambridge, England , 1984.

Mintz, Y., and Y.V. Serafini, A global monthly climatology of soil moisture and water balance, *Clim. Dyn., 8*, 13-27, 1992.

Monteith, J.L., *Vegetation and the Atmosphere*, 278 pp, *vol. 1, Academic*, San Diego, Calif., 1975.

Monteith, J.L., *Vegetation and the Atmosphere*, 439 pp, vol. 2, *Academic*, San Diego, Calif., 1976.

Monteith, J.L., Evaporation and surface temperature. *Q.J.R. Meteorol. Soc., 107*, 1-27, 1981.

Mylne, M.F., and P.R. Rowntree, Deforestation of Amazonia–Modeling the effects of the albedo change, *Clim. Res. Tech. Note 7, 39 pp., Hadley Cent., U.K. Meteorol. Off., Bracknell*, England, 1991.

Namias, J., Persistence of mid-tropospheric circulations between adjacent months and seasons, in *The atmosphere and sea in motion* edited by B. Bolin, pp. 240-248, *Rockfeller Inst. Press*, New York,1958.

Nobel, P.S., Biophysical plant physiology and ecology, 608 pp., W.H. Freeman, San Francisco, Calif., 1983.

Nobre, C.A., P.J. Sellers, and J. Shukla, Amazonian deforestation and regional climate change, *J. Clim., 4*, 957-988, 1991.

Noilhan, J., and S. Planton, A simple parameterization of land surface processes for meteorological models, *Mon. Weather Rev., 117*, 536-549, 1989.

Oglesby, R.J. Springtime soil moisture variability, and North American drought as simulated by the NCAR Community Climate Model I, *J. Clim., 4*, 890-897, 1991.

Pielke, R.A., *Mesoscale Meteorological Modeling*, 612 pp, Academic, San diego, Calif., 1984.

Pielke, R.A., and P.L. Vidale, The boreal forest and the polar front, (submitted to J.G.R.).

Priestley, C.H.B., and R.J. Taylor, On the assessment of surface heat flux and evaporation, *Mon. Weather Rev., 106*, 81-92, 1972.

Ramanathan, V., B. Subasilar, G.J. Zhang, W. Conant, R.D. Cess, J.T. Kiehl, H. Grassl, and L. Shi, Warm pool heat budget and shortwave cloud forcing: A missing physics? *Science, 267*, 499-503, 1995.

Rasmusson, E.M., Atmospheric water vapour transport and the water balance of North America, I, Characteristics of water vapour field, *Mon. Weather Rev., 95*, 403-426, 1967.

Rasmusson, E.M., Atmospheric water vapor transport and the water balance of North America, II, Large-scale water balance investigations, *Mon. Weather. Rev., 96*, 720-734, 1968.

Rasmusson, E.M., A study of the hydrology of eastern North America using atmospheric vapor flux data, *Mon. Weather. Rev., 99*, 119-135, 1971.

Rowntree, P.R , and J.A. Bolton, Simulation of the atmospheric response to soil moisture anomalies over Europe, *Q. J. R. Meteorol. Soc., 109*, 501-526, 1983.

Sarachik, E.S., Tropical sea surface temperature on interactive one-dimensional atmosphere ocean model, *Dyn. Atmos. Oceans, 2*, 445-469, 1978.

Segal, M., R. Avissar, M.C. McCumber, and R.A. Pielke, Evaluation of vegetation effects on the generation and modification of mesoscale circulations, *J. Atmos. Sci., 45*, 2268-2292, 1988.

Sellers, P.J., and F.G. Hall, FIFE in 1992: Results, scientific gains, and future research directions, *J. Geophys. Res., 98*, 19091-19109, 1993.

Sellers, P.J., Y, Mintz, Y.C. Sud, and A. Dalcher, A simple biosphere model (SiB) for use with general circulation models, *J. Atmos. Sci., 43*, 505-531, 1986.

Sellers, P.J., W.J. Shuttleworth, J.L. Dorman, A. Dalcher, and J.M. Roberts, Calibrating the Simple Biosphere Model (SiB) for Amazonian tropical forest using field and remote sensing data, I, Average calibration with field data, *J. Appl. Meteorol., 28*, 727-759, 1989.

Sellers, P.J., J.A. Berry, G.J. Collatz, C.B. Field, and F.G. Hall, Canopy reflectance, photosynthesis, and transpiration, III, A reanalysis using improved leaf models and a new canopy integration scheme,*Remote Sens. Environ., 42*, 187-216, 1992.

Sellers, P.J., et al.,The Boreal Ecosystem-Atmosphere Study (BOREAS): An overview and early results from the 1994 field year, *Bull. Am. Meteorol. Soc., 76*, 1549-1577, 1995.

Smith, E.A., W.L. Crosson, and B.D. Tanner, Estimation of surface heat and moisture fluxes over a prairie grassland, 1, In situ energy budget measurements incorporating a cooled mirror dewpoint hygrometer, *J. Geophys. Res., 97*, 18557-18582, 1992.

Smith, E.A., et al., Area-averaged surface fluxes and their time-

space variability over the FIFE experimental domain, *J. Geophys. Res., 97*, 18599-18622, 1992.
Stull, R.B., An Introduction to Boundary Layer Meteorology,. 666 pp., Kluwer, Norwell, Mass., 1988.
Tennekes, H., A model for the dynamics of the inversion above a convective boundary layer, *J. Atmos. Sci., 30*, 558-567, 1973.
Tiedtke, M., Representation of clouds in large-scale models, *Mon. Weather. Rev., 121*, 3040-3061, 1993.
Troen, I., and L. Mahrt, A simple model of the atmospheric boundary layer; sensitivity to surface evaporation, *Boundary Layer Meteorol., 37*, 129-148, 1986.
Viterbo, P., and A.C.M. Beljaars, An improved land surface parameterization scheme in the ECMWF model and its validation, *J. Clim., 8*, 2716-2748, 1995.
Viterbo, P., and P. Courtier, The importance of soil water for medium-range weather forecasting. Implications for data assimilation, Workshop on Imbalance of Slowly Varying Components of Predictable Atmospheric Motions, World Meteorol. Org., Beijing, China, March 1995.
Wetzel, P.J., and A. Boone, A Parameterization for land-atmosphere-cloud exchange (PLACE): Documentation and testing of a detailed process model of the partly cloudy boundary layer over heterogeneous land, *J. Clim, 8*, 1810-1837, 1995.

J. H. Ball and A. K. Betts, Atmospheric Research, RR 3, Box 3125, Pittsford, VT 05763
A. C. M. Beljaars, M. J. Miller, and P. A. Viterbo, European Centre for Medium-Range Weather Forecasts, Shinfield Park, Reading, RG2 9AX, England.

(Received February 21, 1995; revised June 1, 1995; accepted June 21, 1995.)